

**Kolmogorov turbulence in a random-force-driven Burgers equation**

Alexei Chekhlov and Victor Yakhot

*Program in Applied and Computational Mathematics, Princeton University, Princeton, New Jersey 08544*

(Received 15 November 1994)

The dynamics of velocity fluctuations, governed by the one-dimensional Burgers equation, driven by a white-in-time random force  $f$  with the spatial spectrum  $|f(k)|^2 \propto k^{-1}$ , is considered. High-resolution numerical experiments conducted in this work give the energy spectrum  $E(k) \propto k^{-\beta}$  with  $\beta = \frac{5}{3} \pm 0.02$ . The observed two-point correlation function  $C(k, \omega)$  reveals  $\omega \propto k^z$  with the “dynamic exponent”  $z \approx 2/3$ . High-order moments of velocity differences show strong intermittency and are dominated by powerful large-scale shocks. The results are compared with predictions of the one-loop renormalized perturbation expansion.

PACS number(s): 47.27.Gs

From a theoretical viewpoint, one of the most challenging features of strong hydrodynamic turbulence is an interplay between random almost Gaussian background and coherent ordered structures responsible for deviations from Gaussian statistics. Although coherent structures were visualized in three-dimensional flows as sheets or tubes of high vorticity [1], little is known about their analytic structure, stability and, as a consequence, about their relevance to turbulence dynamics. In two-dimensional systems, the role of coherent structures is much better understood: the flow can be decomposed into two components, the background field having close to Gaussian statistics and coherent, extremely stable point vortices, responsible for strongly non-Gaussian features of the flow [2]. Still, the analytic structure of the vortices and the distributions of their sizes and strengths are not yet understood and this is why the full statistical theory of two-dimensional turbulence does not exist.

The analytic properties of the one-dimensional Burgers equation [3]

$$\frac{\partial v}{\partial t} + \frac{1}{2} \frac{\partial v^2}{\partial x} = \nu_0 \frac{\partial^2 v}{\partial x^2}, \tag{1}$$

subject to initial and boundary conditions, are understood rather well: the flow is dominated by the shocks, leading to  $E(k) \propto k^{-2}$  [3]. Moreover, in some cases, the Burgers equation has a stationary solution. For example, if  $v = -U$  and  $v = U$  at  $x = \infty$  and  $-\infty$ , respectively,  $U(x) = -U \tanh[xU/(2\nu_0)]$ , which describes a single shock of the width  $l \approx \nu_0/U$ . In this particular solution, “fluid” particles, created at the boundaries, are carried towards the center of the shock where they disappear. The shock formation is the most significant dynamic property of the Burgers equation and the shocks were studied in the systems decaying from some initial conditions and driven by the large-scale random noise [4]. In the latter case, the energy spectrum is  $E(k) \propto k^{-2}$  and all velocity structure functions  $S_{2n}(r) = [\overline{u(x+r) - u(x)}]^{2n}$  scale as  $S_{2n}(r) \propto r^1$ , characteristic of the shocks.

A totally different result is found in a system governed by (1) driven by a white-in-time random force  $f(x, t)$  defined by its correlation function:

$$\overline{f(k, \omega) f(k', \omega')} = 2(2\pi)^2 D_0 k^{-\gamma} \delta(k+k') \delta(\omega + \omega') \tag{2}$$

with  $\gamma = -2$  corresponding to thermal equilibrium. Here, in the limit  $k \rightarrow 0$  and  $\omega \rightarrow 0$  the two-point velocity correlation function is given by

$$C(k, \omega) = \int \int \frac{\overline{v(k, \omega) v(k', \omega')}}{2} \frac{d\omega'}{2\pi} \frac{dk'}{2\pi} \propto k^{-\alpha} C\left(\frac{\omega}{k^z}\right) \tag{3}$$

with  $\alpha = z = 3/2$  corresponding to  $E(k) = \text{const}$ . Both exponents  $z$  and  $\alpha$  were evaluated from the theories based on the one-loop renormalized perturbation expansions [5,6] and were confirmed by numerical experiments [6]. In this case, the small-scale forcing was strong enough to prevent formation of the shocks and the  $k^{-2}$  energy spectrum. In recent articles [7], it was shown that computation of the second loops for the  $\gamma = -2$  case does not invalidate the results of the one-loop approximation.

In this work, we are interested in an intermediate case of a system governed by (1) with the forcing function added to the right side defined by the relation (2) with  $\gamma = 1$ . This case is extremely interesting because it corresponds to the “almost” constant energy flux  $\Pi(k)$  in the wave-number space:  $\Pi(k) \propto \ln(k/k_0)$ , where  $k_0$  is the inverse largest allowed scale in the system. Since the analytic structure of (1) resembles that of the Navier-Stokes equations, the Kolmogorov argument leading to  $E(k) \propto k^{-5/3}$  can be applied at least on a superficial level. However, in this case the process of the Kolmogorov spectrum generation should compete with the natural tendency of the Burgers equation towards formation of coherent shocks, thus leading to the most interesting dynamics.

We investigate the fluctuations generated by Eq. (1) with the more general dissipation term  $\nu_0(-1)^{p+1} \partial^{2p} v / \partial x^{2p}$  and driven by the random force  $f(x, t)$ . Numerical results, shown below, correspond to  $p = 6$ , which has been chosen empirically to produce sufficiently sharp uv energy spectrum fall-off. The effect of the hyperdissipation on the solutions of the Burgers equation has been studied in a recent paper [8] and we will not dwell upon this issue here. We will just mention that its use is dictated by desire to have as wide a universal range as possible and is based on the assumption that universal ir properties do not depend on the type of dissipation chosen. To simulate (2), the random force has been assigned in the Fourier space as  $f(k, t) = A_f / \sqrt{\delta t} |k|^{-\gamma/2} \sigma_k$ , where

$\sigma_k$  is a Gaussian random function with  $\overline{|\sigma_k|^2} = 1$  and  $\delta t$  is a time step. The force cutoff  $k_c$  was chosen well inside the dissipation range of the energy spectrum. In the case  $p=1$  the dissipation scale is, according to the relation given above,  $l_d \approx \nu_0/U_0$  where  $U_0$  is the rms velocity of the most energetic shock in the system. Spatial discretization was based on the Fourier-Galerkin pseudospectral method with the nonlinear term computation in the conservative form and de-aliasing procedure based on the 2/3 rule. Temporal discretization included two second-order schemes: Runge-Kutta for restarting and stiffly stable Adams-type scheme described in [9] for serial computations. The spectral resolution employed here was 12 288 including the de-aliased modes. Other parameters were chosen to be  $\nu_0 = 9.0 \times 10^{-40}$ ,  $\delta t = 5.0 \times 10^{-5}$ , and  $A_f = 1.4142 \times 10^{-3}$ . It was carefully tested that this parameter set does lead to the strong coupling in the inertial range  $10 \leq k \leq 600$ , such that the viscous term in the energy equation derived from (1) is negligibly small compared with the corresponding nonlinear term.

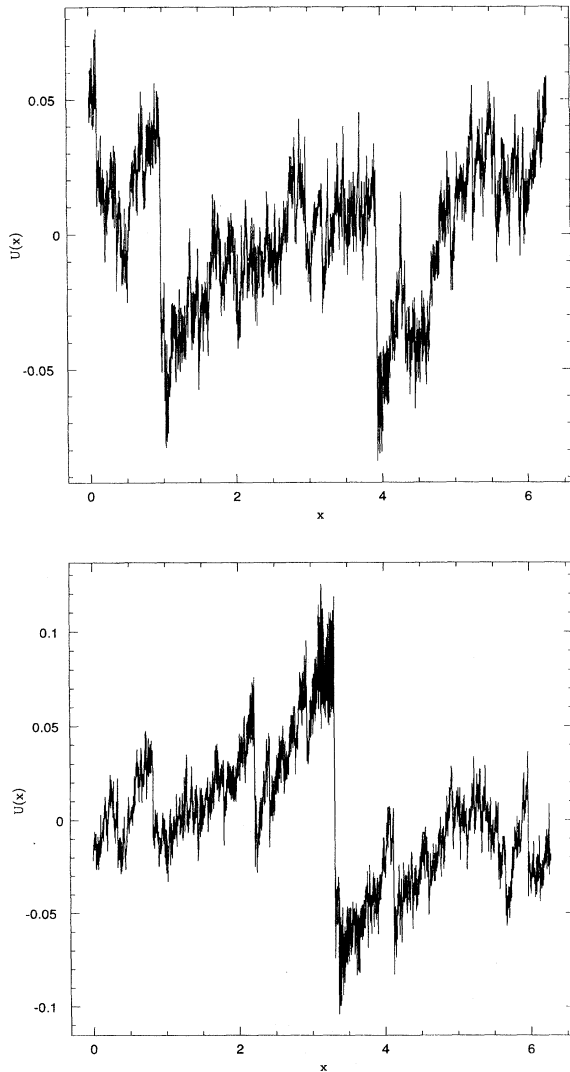


FIG. 1. Solutions  $v(x, t)$  at times  $t=90$  (upper) and  $t=213.5$  (lower).

The results of numerical experiments are presented in Figs. 1–5. Integration was performed for over approximately  $11\tau_{10}$ , where  $\tau_{10} = \pi/V_{rms} \approx 100$  is a largest eddy turnover time. After approximately  $0.5\tau_{10}$  the statistically steady state has been achieved. Figure 1 presents two successive realizations of the velocity field in this steady state. One can see the typical sawtooth structures, characteristic of the dynamical system governed by the Burgers equation. In our case, however, they are superimposed by the random component of the velocity field. It was noticed that the system spends most of the time in the state where there are few (3–4) large-amplitude shocks and many small-amplitude ones. But processes leading to the creation of a single strong shock and its later breakdown into several smaller ones constantly take place. The time evolution of the total energy in the system  $E(t)$  demonstrates strong (with the amplitude of more than 100% of the average energy) fluctuations, characteristic of the instability of the large-scale structures. The time-averaged energy spectrum  $E(k, t)$  [ $E(t) = \int E(k, t) dk$ ], presented in Fig. 2, is well approximated by the Kolmogorov law:  $E(k) \propto k^{-\beta}$  with  $\beta = \frac{5}{3} \pm 0.02$ . The error bars were estimated in the following way: various values of parameter  $\beta$  were used to plot the compensated energy spectrum  $e(k) = k^\beta E(k)$  and only the values of exponent  $\beta$ , for which  $e(k)$  was inside the experimental noise in the entire interval  $10 < k < 600$ , were chosen as representable. The velocity structure functions  $S_{2n}(r) = [\overline{v(x+r) - v(x)}]^{2n}$  are shown in Fig. 3 for  $n=2-4$ . We can see that all  $S_{2n}(r) \propto r^{\beta_{2n}}$  with  $\beta_{2n} \approx 0.91$  indicating that these correlation functions are dominated by coherent shocks. We were not able to detect the logarithmic corrections to the energy spectrum  $E(k)$ . However, the fact that the high-order moments, presented in Fig. 3, are characterized by the exponents close but not exactly equal to unity, indicates that the logarithmic contributions cannot be ruled out. One remarkable result is related to the dissipation rate correlation function presented in Fig. 4,  $G(r) = \overline{\epsilon(x+r)\epsilon(x)} \propto r^{-\mu}$ , with intermittency exponent

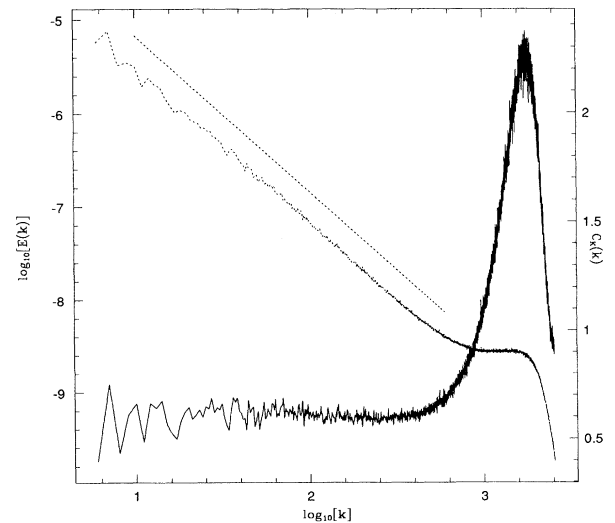


FIG. 2. Dotted curve is the energy spectrum  $E(k)$  (left axis); the straight line above it has the exact slope  $-5/3$ . Solid curve is the compensated energy spectrum  $C_K$  defined in the text (right axis).

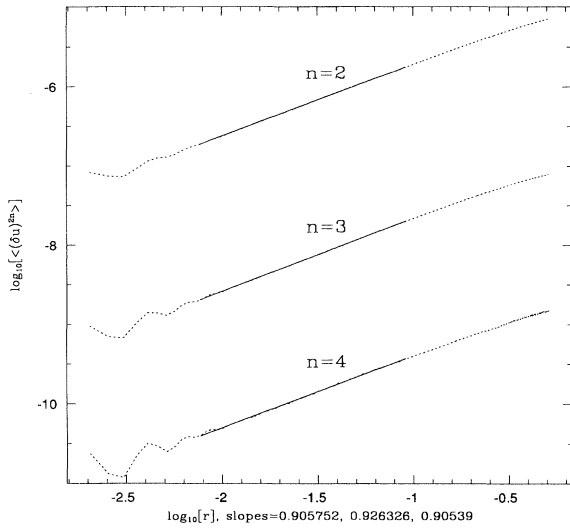


FIG. 3. Velocity differences  $[v(x+r)-v(x)]^{2n}$  for  $n=2, 3, 4$  (dotted curve) with the linear least-squares fit (solid line).

$\mu \approx 0.2 \pm 0.05$  measured inside the universal range  $0.01 \leq r \leq 0.63$ . Note that the dissipation rate correlation function is defined in the physical space and the 2/3 rule de-aliasing procedure was also used for its computation. The obtained value of the dissipation rate exponent  $\mu$  is close to that observed in the experiments on three-dimensional turbulence:  $\mu = 0.25 \pm 0.05$ , see [10], and its general shape resembles the model shape of  $G(r)$  proposed for three-dimensional turbulence in [11]. We would like to emphasize that in the present work the dissipation rate  $\epsilon(x) = \nu_0 (\partial^p v / \partial x^p)^2$  with  $p=6$  strongly differs from the normal viscosity case with  $p=1$ . The fact that the exponent  $\mu$  obtained in this work was close to the one observed in real-life turbulence provides an indication that the correlation function of the dissipation rate for the inertial range values of

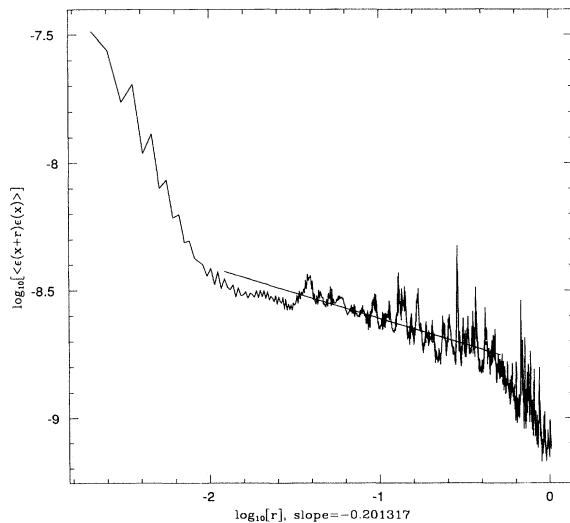


FIG. 4. Energy dissipation correlation function  $\overline{\epsilon(x+r)\epsilon(x)}$  with the linear least-squares fit, giving the intermittency exponent  $\mu = 0.2 \pm 0.05$ .

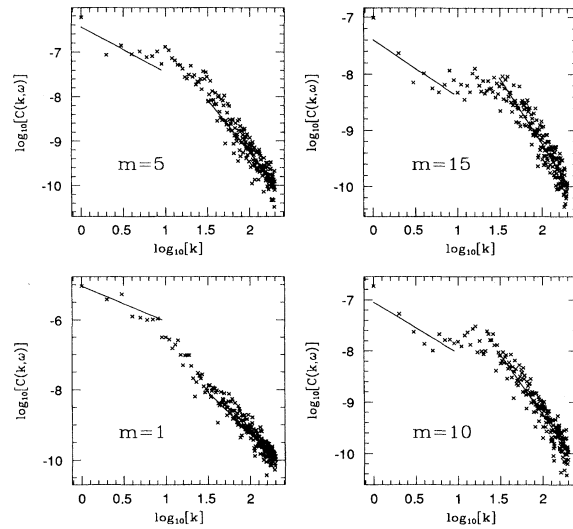


FIG. 5. Points denote the self-correlation function of the solution  $C(k, \omega)$  for fixed frequencies  $\omega = 2\pi m/\tau$  with  $m=1, m=5, m=10, m=15$ , and  $\tau=100.05$ . Solid lines denote the corresponding asymptotics of the one-loop prediction given by (4).

the displacement  $r$  is independent of the structure of the dissipation range. A similar conclusion was reached from the recent numerical experiments of three-dimensional turbulence in [12]. As one can see from Fig. 4, the accuracy of the exponent  $\mu$  is not as good as that of the exponent in the expression for the energy spectrum. In addition, to assess the importance of the result, the role of the hyperviscosity in the dissipation rate correlation function is to be further investigated.

Important information about the dynamics of a nonlinear system can be extracted from the correlation function defined by (3). In the scale-invariant regime, according to the theories based on the one-loop renormalized perturbation expansion [5,6]

$$C(k, \omega) = \frac{D_0 k^{-1}}{\omega^2 + \nu^2(k, \omega=0) k^4}, \quad (4)$$

where  $\nu(k, \omega=0) \approx (3D_0/4\pi)^{1/3} k^{-4/3}$ , corresponding to  $z=2/3$  and  $\alpha=-7/3$  in (3). The frequency dependence of the effective viscosity  $\nu(k, \omega)$  is neglected in the relation (4). This is the direct consequence of the assumption that the dynamics of the inertial range modes  $v(k, \omega)$  are dominated by the “distant interactions” with the modes  $v(q, \Omega)$  with  $|k| \ll |q|$  and can be described by the  $k$ -dependent eddy viscosity. It is clear that this approximation cannot be valid when we are interested in the behavior of the most powerful large-scale structures, because of the strong interaction between them leading to the events of the shock instability observed in this work. The energy spectrum derived from (4) is  $E(k) = \int C(k, \omega) d\omega / (2\pi) = (\pi D_0^2/6)^{1/3} k^{-5/3}$ . The energy flux in the wave-number space can be expressed in terms of the amplitude of the force correlation function  $D_0$  as follows:  $\Pi(k) = \Pi(k_0) + D_0 \ln(k/k_0)$ . Then, the value of the “Kolmogorov” constant arising from (6) is  $C_K = \{[\Pi(k) - \Pi(k_0)]/\}$

$\ln(k/k_0)\}^{-2/3}k^{5/3}E(k)=(\pi/6)^{1/3}$ . The numerical value  $C_K \approx 0.806$  agrees well with the results of numerical simulation; see Fig. 2. As in many other cases, understanding the reasons for a good agreement between the theory, based on the one-loop renormalized perturbation expansion, and experimental data, remains a major challenge.

The computational procedure for  $C(k, \omega)$  included the following steps. Starting from some initial moment  $t=t_0$  well inside the statistically steady state, the solution  $v(k, t)$  was stored at the time instants  $t_j=t_0+Tj/M$ , where  $T=100$  was chosen to be of the order of  $\tau_{t_0}$ . Then at  $t=t_M$  the solution  $v(k, \omega)$  was found via discrete Fourier transform. Repeating such a procedure with time and assuming each realization of  $v(k, \omega)$  to be independent of others, which certainly is only an approximation, one can compute  $C(k, \omega)$  as an average over such realizations. Memory requirements allowed us to keep only 200 first wave vectors and limit ourselves with  $M=3000$ . Results of computations of  $C(k, \omega)$ , presented in Fig. 5, can be compared with the prediction (4). The relation (4) was derived neglecting the infrared divergences resulting in the transport of the small-scale fluctuations by the large-scale coherent structures. This kinematic interaction (“sweeping effect”) can be accounted for by the Doppler shift  $\omega \rightarrow \omega + kV$  in (4), where  $V$  is the characteristic velocity of the large-scale structures. Of major interest is whether  $C(k, \omega)$  is described by (4) or not and whether  $V$  is zero or not. If the sweeping effect is present in the long-time behavior then there are three possible scaling regimes of  $C(k, \omega)$  as  $\omega \rightarrow 0+$ :  $C(k, \omega) \propto k^{-1}$  if  $k \ll (\omega^3/D_0)^{1/2}$ ,  $C(k, \omega) \propto k^{-7/3}$  if  $(\omega^3/D_0)^{1/2} \ll k \ll D_0/V^3$ , and  $C(k, \omega) \propto k^{-3}$  if  $k \gg D_0/V^3$ . It is clear from Fig. 5 that the theoretical prediction (4) is surprisingly accurate in both limits of large and small frequencies  $\omega$ . Only in a narrow intermediate range of the wave numbers  $\omega \approx \nu(k, \omega=0)k^2$  does prediction (4) fail. The flattening of  $C(k, \omega)$  observed in this interval indicates that the scaling function  $F(x)$  in (3) is

a decreasing function of  $x$  when  $x \approx 1$ . The quantitative agreement between theory and simulations in the limit of large wave numbers  $k$  shows that the “sweeping velocity”  $V$  is small. This may be a consequence of the fact that the large-scale shocks are almost steady. We would also like to note that the accuracy of the  $C(k, \omega)$  computation may not be easily increased because of the computer resource limits which have been reached by us. The above result leads to an interesting possibility: The infrared divergences, present in the theory, are not summed up into a mere transfer of small-scale fluctuations by the large-scale structures but are reflected in the creation of a large-scale condensate state, which in this case has a very simple physical meaning as a collection of strong shocks moving with a very small velocity  $V$ . Derivation of the equation of motion describing dynamics of coherent shocks is an important and interesting problem and will be the subject of future communication.

To conclude, the above results, obtained in a simple one-dimensional system, are surprisingly similar to the outcome of experimental investigations of the real-life three-dimensional turbulence. In the one-dimensional case, however, the dynamics and geometrical features of the “turbulence” building blocks are well understood and a cascade process is readily envisioned as a coagulation of the weak and wide shocks (the shock width and its amplitude are related as  $l \approx \nu_0/u$ ) into ever stronger and narrower structures until the dissipation takes over. Moreover, the total dissipation rate in an interval of the length  $r$  is prescribed and is equal to  $\epsilon_r \propto \ln(rU_0/\nu_0)$ . Given these simplifications, one may hope that the full theory of Kolmogorov turbulence in the one-dimensional Burgers equation is not out of reach.

This work was supported by grants from ARPA and AFOSR. Many stimulating discussions with V. Borue, R. H. Kraichnan, S. Orszag, A. Polyakov, and Ya. Sinai are gratefully acknowledged.

- [1] Z.-S. She, E. Jackson, and S. A. Orszag, Proc. R. Soc. London Ser. A **434**, 101 (1991).  
 [2] L. Smith and V. Yakhot, Phys. Rev. Lett. **71**, 352 (1993).  
 [3] J. M. Burgers, *The Nonlinear Diffusion Equation. Asymptotic Solutions and Statistical Problems* (Reidel, Dordrecht, 1974); J. Krug and H. Spohn, in *Solids Far From Equilibrium: Growth, Morphology and Defects*, edited by C. Godrèche (Cambridge University Press, Cambridge, England, 1992).  
 [4] Ya. G. Sinai, Commun. Math. Phys. **148**, 601 (1992); J. Stat. Phys. **64**, 1 (1991).  
 [5] D. Forster, D. R. Nelson, and M. J. Stephen, Phys. Rev. A **16**,

732 (1977).

- [6] V. Yakhot and Z.-S. She, Phys. Rev. Lett. **60**, 1840 (1988).  
 [7] T. Sun and M. Plischke, Phys. Rev. E **49**, 5046 (1994); E. Frey and U. C. Tauber, *ibid.* **50**, 1024 (1994).  
 [8] J. P. Boyd, J. Sci. Comput. **9**, 81 (1994).  
 [9] G. E. Karniadakis, M. Israely, and S. A. Orszag, J. Comput. Phys. **97**, 414 (1991).  
 [10] K. R. Sreenivasan and P. Kailasnath, Phys. Fluids A **5**, 512 (1993).  
 [11] M. Nelkin, Phys. Fluids **24**, 556 (1981).  
 [12] V. Borue and S. A. Orszag, Phys. Rev. E **51**, 856 (1995).